blood advances

American Society of Hematology
2021 L Street NW, Suite 900,
Washington, DC 20036
Phone: 202-776-0544 | Fax 202-776-0545
bloodadvances@hematology.org

CD4+ CAR-T cell exhaustion associated with early relapse of multiple myeloma after BCMA CAR-T cell therapy

Tracking no: ADV-2023-012416R2

Guy Ledergor (University of California, San Francisco, United States) Zenghua Fan (University of California, San Francisco, United States) Kai Wu (University of California, San Francisco, United States) Elizabeth McCarthy (University of California, San Francisco, United States) Axel Hyrenius-Wittsten (University of California, San Francisco, United States) Alec Starzinski (University of California, San Francisco, United States) Hewitt Chang (University of California, San Francisco, United States) Mark Bridge (University of California, San Francisco, United States) Serena Kwek (University of California, San Francisco, United States) Alexander Cheung (University of California, San Francisco, United States) Sophia Bylsma (University of California, San Francisco, United States) Erik Hansen (University of California, San Francisco, United States) Jeffrey Wolf (UCSF, United States) Sandy Wong (University of California, San Francisco, United States) Nina Shah (University of California, San Francisco,) Kole Roybal (Parker Institute of Cancer Immunotherapy, United States) Thomas Martin (UCSF, United States) Jimmie Ye (University of California, San Francisco, United States) Lawrence Fong (Parker Institute of Cancer Immunotherapy, United States)

Abstract:
Multiple myeloma is characterized by frequent clinical relapses following conventional therapy. Recently, chimeric antigen receptor T (CAR-T) cells targeting B-cell maturation antigen (BCMA) has been established as a treatment option for patients with relapsed or refractory disease. However, while >70% of patients initially respond to this treatment, clinical relapse and disease progression occur in most cases. Recent studies showed persistent expression of BCMA at the time of relapse, indicating that immune intrinsic mechanisms may contribute to this resistance. While there were no pre-existing T cell features associated with clinical outcomes, we found that patients with a durable response to CAR-T cell treatment had greater persistence of their CAR-T cells compared to patients with transient clinical responses. They also possessed a significantly higher proportion of CD8+ T effector memory cells. In contrast, patients with short-lived responses to treatment have increased frequencies of cytotoxic CD4+ CAR-T cells. These cells expand in vivo early after infusion but express exhaustion markers (HAVCR2 and TIGIT) and remain polyclonal. Finally, we demonstrate that non-classical monocytes are enriched in the myeloma niche and may induce CAR-T cell dysfunction through mechanisms that include TGFβ. These findings shed new light on the role of cytotoxic CD4+ T cells in disease progression after CAR-T cell therapy.

Conflict of interest: COI declared - see note

COI notes: GL is employed by and holds stock in Caribou Biosciences, Inc.; SW is employed by and holds stock in Bristol Myers Squibb; NS is employed by and owns stock in AstraZeneca, served as a consultant for Amgen, CareDx, CSL Behring, GlaxoSmithKline, Indapta Therapeutics, Karyopharm Therapeutics, Kite, Oncopeptides, and Sanofi, and received research funding from bluebird bio, Bristol Myers Squibb/Celgene, Janssen, Nektar, Poseida, Precision BioSciences, Sutro Biopharma, and TeneoBio; KTR is a co-founder, consultant, scientific advisory board member and stockholder of Arsenal Biosciences, Dispatch Therapeutics, and Moonlight Bio, a consultant and stockholder in Cell Design Labs (now a Gilead Company), holds stock in Gilead, and is an adviser to Venrock; CJY is a co-founder of Survey Genomics, and a scientific advisory board member of Related Sciences and Immunai, a consultant for Maze Therapeutics, TReX Bio, ImYoo, and Santa Ana Bio, and received research support from the Chan Zuckerberg Initiative, Chan Zuckerberg Biohub, Genentech, BioLegend, ScaleBio, and Illumina. TM received research funding from Sanofi, BMS, Janssen and Amgen, and is a consultant for GSK and Pfizer. LF received research funding from Abbvie, Bavarian Nordic, Bristol-Myers Squibb, Dendreon, Janssen, Merck, Nektar, Roche/Genentech and Parker Institute; served as a consultant to Abbvie, Actym, Amgen, Astra Zeneca, Atreca, Bioatla, Bolt, Bristol Myer Squibb, Crescendo, Daiichi Sankyo, Immunogenesis, Innovent, Merck, NGMBio, Nutcracker, RAPT, Senti, Sutro, and Roche/Genentech; and has ownership interests in Actym, Atreca, Bioatla, Bolt, Immunogenesis, Nutcracker, RAPT, and Senti, unrelated to the work here.

Preprint server: No;

Author contributions and disclosures: GL conceived the study, designed and performed experiments and sample acquisition from patients, analyzed data and wrote the manuscript; ZF analyzed scRNAseq data and wrote the manuscript; KW designed and performed experiments of targeted amplification and flow cytometry killing assays, analyzed data and wrote the manuscript; EM analyzed scRNAseq data and performed de novo transcriptome assembly; AHW designed and performed CAR-T transduction and killing assays; AS performed killing assays and flow cytometry experiments; HC performed single cell RNA sequencing library preparation and flow cytometry experiments; SK and AC designed flow cytometry panels; SB, JW, SW, NS recruited patients and provided de-identified clinical data; EH performed bone marrow collection from healthy donors undergoing surgery; KR designed CAR-T killing assays; JY designed experiments and provided guidance on data analysis; TM and LF conceived the study, designed experiments, analyzed data and wrote the manuscript.

Non-author contributions and disclosures: No;

Agreement to Share Publication-Related Data and Data Sharing Statement: Single cell transcriptomic data is available in Gene Expression Omnibus (GEO), accession number GSE246342, Flow cytometry data or additional unidentified patient data will be shared upon request.

Clinical trial registration information (if any):

$CD4^+$ CAR-T cell exhaustion associated with early relapse of multiple myeloma after BCMA CAR-T cell therapy

Guy Ledergor*[1], Zenghua Fan*[1], Kai Wu*[1,], Elizabeth McCarthy[2], Axel Hyrenius-Wittsten[3,4], Alec Starzinski[1], Hewitt Chang[1], Mark Bridge[1], Serena Kwek[1], Alexander Cheung[1], Sophia Bylsma[1], Erik Hansen[5], Jeffrey Wolf[1], Sandy Wong[1], Nina Shah[1], Kole T Roybal[3,6], Thomas Martin*[1], Chun J Ye[2,6], Lawrence Fong*[1,6,7]

1. Helen Diller Family Comprehensive Cancer Center, UCSF; 2. Institute for Human Genetics, UCSF; 3. Microbiology and Immunology, UCSF; 4. Division of Clinical Genetics, Department of Laboratory Medicine, Lund University; 5. Department of Orthopedic Surgery, UCSF; 6. Parker Institute for Cancer Immunotherapy; 7. Fred Hutchinson Cancer Center.

*These authors contributed equally

Corresponding author: Lawrence Fong, MD; lawrence.fong@fredhutch.org; (415) 514-3160

Data Sharing: Single cell transcriptomic data is available in Gene Expression Omnibus (GEO), accession number is GSE246342. Flow cytometry data or additional unidentified patient data will be shared upon request.

Text word count (excluding abstract, acknowledgments, references): 3,831

Abstract word count: 206

Number of figures and tables: 5 main figures, 2 tables

Number of references: 47

Key Points

- Despite the high initial rates of response to anti-BCMA CAR-T cell therapy in myeloma, those responses are frequently short-lived.
- Exhausted CD4+ CAR-T cells, identified by single cell assays in the patients' blood and marrow, is linked to early relapse.
- Myeloid cells in the myeloma niche blunt CD4+ CAR-T killing via TGFβ.

Abstract

Multiple myeloma is characterized by frequent clinical relapses following conventional therapy. Recently, chimeric antigen receptor T (CAR-T) cells targeting B-cell maturation antigen (BCMA) has been established as a treatment option for patients with relapsed or refractory disease. However, while >70% of patients initially respond to this treatment, clinical relapse and disease progression occur in most cases. Recent studies showed persistent expression of BCMA at the time of relapse, indicating that immune intrinsic mechanisms may contribute to this resistance. While there were no pre-existing T cell features associated with clinical outcomes, we found that patients with a durable response to CAR-T cell treatment had greater persistence of their CAR-T cells compared to patients with transient clinical responses. They also possessed a significantly higher proportion of CD8+ T effector memory cells. In contrast, patients with short-lived responses to treatment have increased frequencies of cytotoxic CD4+ CAR-T cells. These cells expand *in vivo* early after infusion but express exhaustion markers (*HAVCR2* and *TIGIT*) and remain polyclonal. Finally, we demonstrate that non-classical monocytes are enriched in the myeloma niche and may induce CAR-T cell dysfunction through mechanisms that include TGFβ. These findings shed new light on the role of cytotoxic CD4+ T cells in disease progression after CAR-T cell therapy.

Introduction

Multiple myeloma (MM), a plasma cell neoplasm, accounts for 10% of hematological malignancies in developed countries[1]. Despite considerable advances in the last , it remains largely incurable, and relapse is considered an inevitable part of the disease course[2,3]. B cell maturation antigen (BCMA) has emerged as a promising therapeutic target in myeloma in the relapse/refractory (RRMM) setting[4]. BCMA is expressed preferentially by mature B lymphocytes and plasma cells[5]. Due to its specificity, BCMA has been an attractive candidate to be targeted by chimeric antigen receptor T (CAR-T) cells[6–9]. These genetically modified T cells express anti-BCMA single chain variable fragment (scFv) linked to co-stimulatory and signaling domains, and upon binding to cell surface BCMA, activation followed by effector function leads to lysis of myeloma cells[10]. Despite the promising results achieved by anti-BCMA CAR-T in RRMM in terms of response rates, the absence of durable remissions is common[11]. Possible reasons for this phenomenon include CAR-T cell intrinsic qualities such as expansion capacity and T cell exhaustion/dysfunction cell state, in addition to CAR-T cell-extrinsic factors like antigen escape and immune suppression by the hostile bone-marrow microenvironment[12,13]. However, previous studies have demonstrated that the immune microenvironment might dictate the response to bispecific T cell engager antibodies, but not to CAR-T cells[14]. To gain insight into the factors involved in long term response to anti-BCMA CAR-T in RRMM and functional high-risk MM, we performed single cell sequencing of 690,939 T cells, coupled with T cell receptor (TCR) clonality assessment, and additional 227,420 non-B non-T immune cells from the myeloma niche, in a longitudinal fashion from n=15 patients (78 samples, mean 5 samples per patient), who had received anti-BCMA CAR-T cell therapy; and 5 age-matched control subjects. We developed a computational method to identify anti-BCMA CAR-T cells *in silico* and by targeted sequencing, and show that in patients with an early relapse, CD4+ CAR-T cells *in vivo* express cytotoxicity and exhaustion markers and have a polyclonal TCR profile.

Methods

Human patients and subjects

This study was approved by the UCSF IRB, according to the principles in the declaration of Helsinki. All subjects were provided written informed consent (IRB#10-00545). The patients were enrolled in 4 clinical trials

of lentiviral-transduced 4-1BB anti-BCMA CAR-T (NCT02658929, NCT03274219, NCT03430011 and NCT03361748), and the summary of their characteristics is presented in Table 1. Table 2 provides detailed characteristics by patient.

Processing of human bone marrow and peripheral blood samples

Bone marrow (BM) aspirates were diluted 1:1 in FACS buffer (PBS with 0.1% BSA and 2 mM EDTA). Peripheral blood (PB) samples were diluted 1:2 in FACS buffer. Mononuclear cell separation was performed by density centrifugation (Ficollpauqe, GE) with diluted BM cells (centrifugation for 25 min, 500g). Cells were manually aspirated and washed with FACS buffer (5 min at 450g). Red blood cells were lysed using RBC lysis buffer (Invitrogen) for 5 min at 4°C. BM cells were washed (5 min, 300g), resuspended in FACS buffer, and kept on ice.

Cell sorting

Within 1 hour after processing, cells were stained with Total-Seq C antibodies (BioLegend) and flow cytometry antibodies, including biotinylated BCMA protein (Acro Biosystems) followed by streptavidin. Cells were sorted (Aria Fusion, BD) based on FSC, SSC, CD45+ CD19- CD3+ (T cells) and CD45+ CD19- CD3- (nonB nonT cells) (Figure S1).

Single-cell library preparation

Sorted cells were washed, counted and loaded onto Chromium platform (10x Genomics) with the Single Cell 5' v1 kit with up to 50,000 cells per well. Libraries were sequenced using Illumina NovaSeq 6000.

Single-cell transcriptional analyses

Raw single cell data was processed by Cell Ranger (version 5, GRCh38). Doublet detection was performed on the filtered gene expression matrices using DoubletDetection[15] with default parameters, and then analyzed by Scanpy pipeline[16], as previously described[17]. Principle component analysis (PCA) was performed with top 50 principal components, followed by sample-wise batch correction Combat[18] and Harmony[19], Leiden clustering[20]

and UMAP plotting[21]. Annotation of each unbiased population was performed by manual inspection of the top-ranked genes of each cluster. Analysis of cell density was carried out by Scanpy. ANOVA with Tukey's HSD test was performed followed by Benjamini-Hochberg (BH) adjustment.

For nonB nonT cells, to decrease batch effects, we performed "*in* silico sorting" for CD14. The expression of CD14 was measured by both frequency distribution density plot and two-axis plot of CD14 versus CD16. Then a threshold of 0.6 was set to retain only CD14+ cells. Raw expression matrix of CD14+ cells was extracted and processed in the same manner followed by Leiden clustering.

Single-cell TCR analysis

scRNA-seq reads were processed by Cell Ranger VDJ. For each cell barcode, the TRA or TRB clonotype with most abundant UMIs was selected. Clones with either α chain or β chain or paired α:β chains by amino acid sequences were kept for downstream analysis. Expanded clones were defined as >1 cell with the same clonotype. Gini coefficient was calculated using ineq in R[22]. Only cells with matched cell barcodes from scRNA-seq reads were used. Comparison of Gini coefficients were carried out by Wilcoxon rank sum test followed by BH adjustment. When assessing clones longitudinally, only paired patients that have both pre- and post-treated samples were included.

Differential gene expression analysis

Differential gene expression (DGE) analysis was performed using DESeq2 in R[23]. For each gene, the raw counts in CD4 CAR-T cells (from CD4 Tnaïve and CD4 Tem clusters) with low CD8 expression, from each sample were aggregated as one value to represent this sample. The matrix of gene by sample was used for comparison between durable responders (DR) and transient responders (TR). The same was done for CD8 CAR-T cells (CD8 GZMB+ Tem, CD8 GZMK+ Trm, CD8 GZMB+ Teff, GNLY+ T, and CD8 Tnaive clusters). Significant genes were selected as p-value<0.05 and fold-change >1.5.

DGE analysis was also performed using MAST[24], a generalized linear model tailored for scRNA-seq data, while the number of genes detected per cell was controlled as a covariate. Multiple test adjustment was

performed using p.adjust function in R by controlling false discovery rate. Significant genes were selected as adjusted p-value<0.05 and fold-change >1.5.

Targeted amplification of cDNA libraries for CAR-T detection

To annotate CAR-T cells, targeted amplification was employed on cDNA libraries generated from 10x scRNA-seq platform. Lentiviral specific transcripts expressed from bulk RNAseq data were identified. Reverse primer (5'GTGACTGGAGTTCAGACGTGTGCTCTTCCGATCTTGTTTCTTTCCCCCTGGCCTTAAC) that is compatible with the 10x Genomics 5' V1 kit was designed to selectively amplify CAR-specific transcript from cDNA libraries, while preserving UMI and cell barcodes. Twenty ng of cDNA libraries were linearly amplified using reverse primer only, followed by purification using SPRI-select beads at 1.5X (Beckman Coulter), followed by 35 cycles of PCR using target-specific reverse primer and universal forward primer (10x Genomics). We performed sample indexing and attachment of flow cell binding sequences using SI PCR primer and I7 index primers. The NGS libraries were pooled and sequenced on MINIseq with 300-cycle kit (Illumina).

CAR-T cells annotation from targeted sequencing data

CAR-T cells were identified from targeted amplification sequencing data of the lentiviral GAG gene. The sequence CGAATTTTTTCCCATTTATCTAATTCTCCCCCGCTTAATACCGACGCTCTCGCACCCTAC was found on Read 2 (R2), followed by extraction of cell barcodes (1-16nt), and UMI sequence (17-26nt) and calculating the UMI count in each unique cell barcode. UMI count per cell for GAG- cells was performed in the same manner. Then the UMI/cell distribution was plotted and examined for GAG+ and GAG- cells (Fig S2). The threshold UMI/cell ≥ 2 was selected to define CAR-T cells.

CAR-T cell annotation of fully humanized CAR-T with modified lentiviral genes

For *in silico* CAR-T cell identification, we flow-sorted a humanized CAR-T cell sample and created full-length cDNA libraries using SMART-Seq[25]. We then created a *de novo* transcriptome assembly using Trinity[26] v.2.9.1. From the resulting transcriptome, we identified one CAR transcript based on it containing a 3' viral UTR

sequence “TGGAAGGGCTAATTCACTCCCAAAGAAGACAAGAT”. We used Kallisto[27] v.0.46.0 to align each scRNA-seq read to the *de novo* transcriptome generated by Trinity. We identified CAR-T cells as cells with more than zero (>0) counts of the associated CAR transcript.

CAR-T cell scores

Activation score was calculated by Scanpy function ‘scanpy.tl.score_genes’ with this gene signature: *PDCD1*, *CTLA4*, *HAVCR2*, *LAG3*, *ENTPD1*, *TOX*, *LAYN*, *CD160*, *CD244*, *TIGIT*, while cytotoxicity score was calculated in the same way by this gene signature: *NKG7*, *PRF1*, *GZMB*, *GZMK*, *TNF*, *IFNG.*

Cell interaction analysis

To explore cell-cell communications between non-classical monocyte population and early stage (day 14 and day 30) CD4+ and CD8+ CAR-T cells, CellphoneDB[28] v2 was performed by the function ‘statistical_analysis’ with default parameters. Only significant gene pairs by default threshold from the output ‘significant_means.csv’ were visualized by heatmap with Python package Seaborn[29].

Enrichment scores for IFNγ and TGFβ pathways

Pathway enrichment analysis on differentially expressed (DE) genes was performed using GSEA[30] 4.2.3. The DE genes of CD4+ CAR-T cells between DR and TR groups were ranked by “-log(p value) fold change” and analyzed using “GSEA PreRanked” tool. Analysis was performed using MsigDB with 1000 permutations. FDR < 0.25 was selected as cutoff for statistical significance.

Co-culture with re-stimulation

We generated anti-BCMA CAR-T cells as previously described[31], with BCMA-50 scFv sequence[32], CD8 hinge and transmembrane domain, 4-1BB co-stimulatory domain, CD3ζ, T2A and EGFP. Lentivirus containing the construct was produced, concentrated, and titrated as previously described[31]. CD4+ T cells were isolated from apheresis collections of 2 healthy donors using CD4 negative selection kits (STEMCELL Technologies) and were viably frozen in media containing 10% DMSO. CD4+ T cells were thawed and stimulated for 24 hours

using anti-CD3/CD28 Dynabeads (Thermo Fisher) before lentiviral transduction. 72 hours after transduction, CAR-T cells were sorted based on EGFP levels. On Day 7, CD4+ CAR-T cells were co-cultured with the target myeloma cell line, MM1.S expressing RFP, at effector:target (E:T) ratio of 1:4 with or without 10ng/ml recombinant human TGFβ (R&D Systems). Fresh media were re-supplanted every 3 days. During the co-culture, cells were counted and E:T ratio was assessed by comparing the GFP+ and RFP+ population every 3 days, fresh target cells were fed when E:T ratio was higher than 1:1. After 3-week co-culture, CD4+ CAR-T cells were isolated and the purity of CAR T cells were evaluated by fluorescence microscopy before subsequent assays.

In vitro killing assay

MM1.S and OCI-AML3 cancer cell lines were used as target cells and negative control, respectively. Target and negative control cells were first stained with Calcein AM Viability Dye (Thermo Fisher). Then, 15,000 target or negative control cells were seeded with or without 2,500 CD4+ CAR-T cells (E:T ratio = 1:6) at a final volume of 200μL in a 96-well U-bottom plate. After 24-hour incubation, Aurora Full Spectrum Flow Cytometry (Cytek Biosciences) was used to determine the number of calcein+ cells (live target or negative control cells) and EGFP+ cells (CD4+ CAR-T cells). Cancer cell killing by CD4+ CAR-T cells was calculated using the following formula, where α is the mean of calcein+ cell counts from wells containing cancer cells only (no CAR-T), while β and γ represent the number of calcein+ and EGFP+ cells from each sample well, respectively:

$$\%\, normalized\ cancer\ cell\ killed\ = \left(\frac{-\alpha-\beta}{\gamma}\right)\times 100\%$$

3 technical replicates were performed for each condition, and for each donor.

This study was approved by the University of California, San Francisco Institutional Review Board, according to the principles in the declaration of Helsinki. All patients and healthy donors undergoing hip replacement surgery were provided written informed consent for genomic sequencing and review of electronic medical records (IRB#10-00545). The patients were enrolled in 3 clinical trials of lentiviral-transduced anti-BCMA CAR-T containing a 4-1BB co-stimulatory domain. Patients were enrolled in clinical trials NCT02658929, NCT03274219 and NCT03430011

Results

Myeloma bone marrow niche is enriched with GZMB CD8+ T effector cells

To understand the cell state of T cell states in myeloma patients, we collected bone marrow (BM) and peripheral blood (PB) samples at baseline (prior to lymphodepletion), and longitudinally following infusion (78 samples from 15 patients, median 3 additional time points). Additionally, T cells from 5 subjects undergoing hip replacement surgery due to isolated osteoarthritis, were collected in the operating room. We performed fresh sorting (within 4 hours from sample collection) of CD45+ CD19- CD3+ lymphocytes (methods, Fig. S1). Freshly sorted cells were subjected to 10x Genomics microfluidic platform for single cell gene expression, coupled with TCR and oligo-labeled surface marker antibodies[33–35] (CITEseq, methods). Following removal of doublets and filtering, 690,939 T-cells were clustered. Cell state annotation was performed according to canonical markers, and revealed 14 different T cell states[36] (Fig. 1A). Representative genes of the different cell states include granzymes (cytotoxicity), *CCR7* (naïve), *FOXP3* (regulatory T cells) and *MKI67* and *TOP2A* (proliferation or cycling) (Fig. 1B). To compare the patients to the hip replacement subjects, we generated density dimensionality reduction map (Fig. 1C) and compared the cell fractions of each group within every cluster[21] (Fig. 1D). MM patients were enriched in the GZMB CD8+ T effector cell cluster, while hip replacement subjects were enriched in CD4 naïve cluster. Heatmap of selected genes shows a preferential expression of exhaustion markers (*CD70*, *CD38*, *HAVCR2*, *LAG3*, *IL2RA*) in T cells derived from MM patients (Fig. 1E).

CAR-T cells annotation, cell states and clonality

To understand the specific cell states of CAR-T cells, we identified them using a combination of two methods (methods, Fig. 2A): *In silico* generation of a *de novo* transcriptome from full-length RNA-seq reads (for CAR-T containing modified lentiviral genes), and a targeted amplification of integrated lentiviral genes (for CAR-T containing unmodified lentiviral genes). 100,157 CAR-T cells were identified from all 15 patients across different time points (Fig. 2B). Single cell CAR-T annotation correlated with flow cytometry staining for the CAR-T cells (Fig. S1). The fraction of CD8+ CAR-T cells predominated up to 30 days post-infusion, regardless of product used (Fig. 2C). CD4+ CAR-T naïve cells were enriched in hip replacement subjects ($p < 0.027$,

0.00084), while CAR-T cells and non-CAR-T cells from myeloma patients were enriched for GZMB CD8+ effector T (p = 0.027, 0.015). There was no statistically significant difference in the distribution of CD8+ effector CAR-T and CD4+ CAR-T cells (naive or effector memory) for patients dosed with different CAR-T cell products (Fig. S1F). Surprisingly, the Gini index (correlated with TCR clonality), was lower for both CD4+ and CD8+ CAR-T cells when compared to non-CAR-T cells[37,38] (p = 0.0064 and p < 0.001, respectively) (Fig. 2E, Fig. S2). Comparing expanded clones (≥2 cells with the same TCR sequence) in CAR-T cells reveals that CD8+ CAR-T are more clonally expanded compared with CD4+ CAR-T cells (p < 0.001) (Fig 2F).

Longitudinal analysis of CAR-T cells *in vivo* according to clinical outcome

To probe into the differences and similarities between patients with an early relapse compared to those with durable remissions following CAR-T infusion, we divided the patients into 2 groups: Transient responders (TR) and durable responders (DR). Response was assessed by IMWG criteria. To classify patients into DR group, the 6 months mark was used, for which the patient has maintained at least a partial response, without rising involved light chains or conversion to minimal residual disease (MRD) positivity. Patients were generally heavily pre-treated, with a median 6 lines of prior anti-myeloma therapies (Table 1). Involved serum free light chain levels were increased in patients in the TR group at day 180 (p = 0.0113) (Fig. 3A). Overall, CAR-T cells were heterogenous, with a representation in all the T cell clusters (Fig. 3B and 3D). In the TR group, CAR-T cells were decreased on days 90 and 180 more than 100-fold, while DR group decreased by less than 1-fold on day 90 and more than 100-fold on day 180 (Fig. 3C). CAR-T cells in DR group were enriched for CD8+ effector memory cell states (p = 0.030) (Fig 3D). We compared the differential gene expression between DR and TR groups in both CD4+ and CD8+ CAR-T cell compartments[23] (methods). While in the CD8+ compartment only *HAVCR2* gene (encoding for TIM3) was significantly elevated in the TR group (p = 0.00011, $Log_2FC = 1.1$) , in the CD4+ compartment both *HAVCR2* and *TIGIT* were significantly increased (p < 0.001, $log_2FC = 1.8$ and p < 0.001 , $log_2FC = 1.6$, respectively), along with cytotoxicity markers *NKG7* and *PRF1* (p = 0.0013 and p < 0.001, respectively) in the TR group (Fig. 3E, 1F).

Exhausted cytotoxic CD4+ CAR-T cells are associated with transient, short-lived clinical response

To elucidate the nature of cytotoxic and exhaustion genes of the CAR-T cells, we calculated the cytotoxicity score and exhaustion score for every annotated CAR-T cell (methods). Plotting single CAR-T cell scores in density maps for the two groups of patients reveals that in TR patients early post-infusion (14-30 days), there was an enrichment of CD4+ cytotoxic exhausted cells compared to DR patients (Wilcoxon rank-sum test, p = 0.0303), unlike the CD8+ compartment (Wilcoxon rank-sum test, p = 0.196) (Fig. 4A and 4B). There was no difference in the exhaustion or cytotoxicity profile of non-CAR resident CD4+ (p = 0.392) or CD8+ T cells (p = 0.26) (Fig. S2).

CAR-T regulatory cells (CAR-Tregs) in the infusion products were recently reported to be associated with relapse of large B-cell lymphoma after anti-CD19 CAR-T cell therapy[39,40]. Since CAR-Tregs are CD4+, we wondered if the association between CD4+ CAR-T cells and early relapse in our myeloma cohort could be attributed to CAR-T regs. We found that CAR-Tregs proportion was not increased in the TR group (Fig. 4C). We further identified the exhausted cytotoxic CD4+ CAR-T cells as either naïve or effector-memory cells, enriched in IFNG signature (normalized enrichment score -1.33, p < 0.001, FDR = 0.082) (Fig. 4D). Differential gene expression analysis confirmed the enrichment of specific IFNG pathway genes (*IFNGR1*, *IFNGR2*, *JAK1*, *STAT1*, *IRF1*) in the TR group (Fig. 4E).

TGFβ contributes to CD4+ CAR-T cell exhaustion

To understand if other immune cells in the myeloma niche affect CAR-T cell state or their ability to kill myeloma cells, we performed fresh sorting of CD45+ CD19- CD3- cells from the BM of both hip replacement subjects and myeloma patients undergoing CAR-T cell therapy. We performed *in silico* sorting of CD14+ cells (Fig. S2) and clustered the cells following filtering and batch correction (methods). CD14+ cells in the BM were comprised of 11 clusters, including classical and plasmacytoid dendritic cells, CD163+ macrophages, 5 different monocyte subtypes expressing *VCAN*, *FCN1* and *S100A8* along with CD68+ CD16+ non-classical monocytes (Fig. 5A and 5B). Non-classical monocytes were enriched in myeloma patients receiving CAR-T cell therapy compared to hip replacement subjects (p = 0.0052 for DR, p = 0.0041 for TR) (Fig. 5C). There was no difference in the frequency of CD14+ cell clusters between the TR and DR groups of patients. As non-

classical monocytes were preferentially present in BM samples of myeloma patients, we simulated their interaction with annotated CAR-Ts[28] (methods). Interaction maps of the CD4+ CAR-T cells with non-classical monocytes in TR and DR groups reveals a possible role for TGFβ axis, with interaction of *TGFB1* in MM-associated non-classical monocytes with *TGFBR3* in CD4+ CAR-T cells (Fig. S2). We then computed the enrichment score of TGFβ pathway in CD4+CAR-T cells and found that the CD4+ CAR-T cells from TR group were enriched for TGFβ related genes (normalized enrichment score = -1.39, p = 0.01, FDR = 0.055) (Fig. 5D). Additionally, *TGFBR2* and *TGFBR3* were preferentially expressed at the single cell level in CD4+ CAR-T cells in the TR group (Fig. 5E). To assess the role of TGFβ in tumor cell killing of CD4+ CAR-T cells, we performed a killing assay with home grown anti-BCMA CAR-T (4-1BB CD3ζ) from 2 healthy donors, after CD4 selection (methods). We used a repetitive stimulation assay with a myeloma cell line to induce CAR-T cell exhaustion *in vitro* (Fig. 5F, methods). We found a significantly decreased cytotoxicity of the CD4+ CAR-T cells compared to control after 3-week co-culture (mean decrease in killing capacity for Donor 1 and Donor 2, 54% and 39%, respectively, $p < 0.001$, student's t-test) (Fig. 5G). TGFβ-treated CAR-T cells expressed multiple exhaustion markers (PD1, TIM3 and CD39) compared to control at the end of the re-stimulation (mean fraction of cells 36.3% vs. 4.7%, p = 0.016, student's t-test) (Fig. 5H). The CAR T cells expressing exahustion markers were functionally exhausted, with hampered secretion of key cytokines IFNγ and TNFα (Fig. S2J). In addition, we find that TGFβ significantly reduces proliferation (assessed by Ki-67 flow cytometry staining) at 1 week of co-culture and persists at 3 weeks post co-culture (Fig. S2K).

Discussion

This study is the largest (to our knowledge) single-cell analysis of anti-BCMA CAR-T cells *in vivo*, with more than 1.1 million single cells analyzed from 15 patients and 5 healthy donors. Rather than focusing on the infusion products, we assayed the CAR-T cells and their microenvironment in the myeloma niche. Our results suggest that specific subtypes of CAR-T cell states early post-infusion contribute to the variability in response to anti-BCMA CAR-T cell therapy in patients with relapsed refractory and functional high-risk MM. Unlike previous studies focusing on single-cell analysis of CD8+ CAR-T cells[41,42], this extensive database of freshly sorted CAR-T cells and immune niche cells sheds light on the role of cytotoxic-like CD4+ CAR-T cells.

Cytotoxic CD4+ TILs have been described in the setting of solid tumors, interacting with other microenvironment cells[43]. In the setting of CAR-T cells, increased CD4:CD8 ratio in the infusion product is associated with better expansion and clinical outcomes[7]. Surprisingly, we have found that across three different products, CD4+ CAR-T cells expressing cytotoxic and activation markers were associated with a worse clinical outcome and early relapse. Unlike previous cases described for anti-CD19 CAR-T in patients with chronic lymphocytic leukemia, our single cell TCR analysis of early post-infusion suggests that anti-BCMA CD4+ CAR-T cells are polyclonal[44]. *In vivo* tracking of CAR-T cells reveals that at days 90 and beyond post-infusion there is no persistence in the patients who have had transient response, compared to those with durable responses. The association between early expansion of exhausted cytotoxic and polyclonal CD4+ CAR-T and transient response or early relapse, requires prospective validation. However, our study introduces the importance of cell states *in vivo* as possible predictors of outcome after CAR-T cell therapy, which constitutes a clinical unmet need. In this context, the relevant exhaustion co-expressed markers are TIM3 and TIGIT (rather than other canonical markers of exhaustion like PD-1 or CTLA-4), which might inform future combination therapeutic approaches.

Our analysis of immune cells in the BM uncovers non-classical monocytes, which are preferentially present in the myeloma niche compared to age-matched controls. Single-cell interaction analysis points to a possible role of the TGFβ axis in the interaction of CD4+ CAR-T cells with these non-classical monocytes. *In vitro* modeling of CAR-T cell exhaustion also demonstrates that TGFβ represents a T cell extrinsic mechanism contributing to T cell exhaustion beyond repetitive antigen stimulation. This finding further corroborates the negative impact of TGFβ on immunotherapy in the tumor microenvironment and makes the case for future research of TGFβ-negating armoring strategies[45,46].

Strengths of this study include 1) large data set comprising of 1.1 million single cells from patients transfused with anti-BCMA CAR-T cells containing 4-1BB co-stimulatory domain; 2) fresh tissue sampling with immediate processing and sorting to minimize stress-induced activation, in conjunction with clonal assessment and cell surface marker analysis. A limitation in our study is the inability to analyze the cell states of the infusion product

and compare those to the ones found *in vivo*. However, as patient-to-patient variability can affect the expansion of CAR-T cells and their cell states, the *in vivo* analysis early post-infusion might be a predictor of long-term outcomes.

Acknowledgements

We thank the patients and their families, the Parnassus Flow Cytometry CoLab (PFCC) and the Human Genetics CoLab. We thank Ajai Chari for critical review of the manuscript.

This work was supported by the Parker Institute of Cancer Immunotherapy and NIH grant R35CA253175. We also acknowledge support from the PFCC (RRID:SCR_018206) supported in part by Grant NIH P30 DK063720 and by the NIH S10 Instrumentation Grant S10 1S10OD021822-01.

Authorship contributions

GL conceived the study, designed and performed experiments, analyzed data and wrote the manuscript; ZF analyzed scRNAseq data and wrote the manuscript; KW designed and performed experiments of targeted amplification and flow cytometry killing assays, analyzed data and wrote the manuscript; EM analyzed scRNAseq data; AHW designed and performed CAR-T transduction and killing assays; AS performed killing assays and flow cytometry experiments; HC performed scRNA-seq library preparation and flow cytometry experiments; MB analyzed scRNAseq data; SK and AC designed flow cytometry panels; SB, JW, SW, NS recruited patients and provided de-identified clinical data; EH performed bone marrow collection from healthy donors undergoing surgery; KTR designed CAR-T killing assays; CJY designed experiments and provided guidance on data analysis; TM and LF conceived the study, designed experiments, analyzed data and wrote the manuscript.

Data availability and sharing statement

Single-cell transcriptomic data is available in Gene Expression Omnibus, accession GSE246342. Flow cytometry data or additional unidentified patient data will be shared upon request.

Conflict-of-interest disclosures

GL is employed by and holds stock in Caribou Biosciences, Inc.; SW is employed by and holds stock in Bristol Myers Squibb; NS is employed by and owns stock in AstraZeneca, served as a consultant for Amgen, CareDx, CSL Behring, GlaxoSmithKline, Indapta Therapeutics, Karyopharm Therapeutics, Kite, Oncopeptides, and Sanofi, and received research funding from bluebird bio, Bristol Myers Squibb/Celgene, Janssen, Nektar, Poseida, Precision BioSciences, Sutro Biopharma, and TeneoBio; KTR is a co-founder, consultant, scientific advisory board member and stockholder of Arsenal Biosciences, Dispatch Therapeutics, and Moonlight Bio, a consultant and stockholder in Cell Design Labs (now a Gilead Company), holds stock in Gilead, and is an adviser to Venrock; CJY is a co-founder of Survey Genomics, and a scientific advisory board member of Related Sciences and Immunai, a consultant for Maze Therapeutics, TReX Bio, ImYoo, and Santa Ana Bio, and received research support from the Chan Zuckerberg Initiative, Chan Zuckerberg Biohub, Genentech, BioLegend, ScaleBio, and Illumina. TM received research funding from Sanofi, BMS, Janssen and Amgen, and is a consultant for GSK and Pfizer. LF received research funding from Abbvie, Bavarian Nordic, Bristol-Myers Squibb, Dendreon, Janssen, Merck, Nektar, Roche/Genentech and Parker Institute; served as a consultant to Abbvie, Actym, Amgen, Astra Zeneca, Atreca, Bioatla, Bolt, Bristol Myer Squibb, Crescendo, Daiichi Sankyo, Immunogenesis, Innovent, Merck, NGMBio, Nutcracker, RAPT, Senti, Sutro, and Roche/Genentech; and has ownership interests in Actym, Atreca, Bioatla, Bolt, Immunogenesis, Nutcracker, RAPT, and Senti, unrelated to the work here.

References

1. Kyle RA, Rajkumar SV. Multiple Myeloma. *N Engl J Med*. 2004;351(18):1860-1873. doi:10.1056/NEJMra041875

2. Palumbo A, Anderson K. Multiple Myeloma. *N Engl J Med*. 2011;364(11):1046-1060; 1060. doi:10.1056/nejmra1011442

3. Egan JB, Shi CX, Tembe W, et al. Whole-genome sequencing of multiple myeloma from diagnosis to plasma cell leukemia reveals genomic initiating events, evolution, and clonal tides. *Blood*. 2012;120(5):1060-1066; 1066.

4. Shah N, Chari A, Scott E, Mezzi K, Usmani SZ. B-cell maturation antigen (BCMA) in multiple myeloma: rationale for targeting and current therapeutic approaches. *Leukemia*. 2020;34(4):985-1005. doi:10/gh288t

5. Carpenter RO, Evbuomwan MO, Pittaluga S, et al. B-cell Maturation Antigen Is a Promising Target for Adoptive T-cell Therapy of Multiple Myeloma. *Am Assoc Cancer Res*. 2013;19(8):2048-2060; 2060. doi:10.1158/1078-0432.ccr-12-2422

6. Brudno JN, Maric I, Hartman SD, et al. T Cells Genetically Modified to Express an Anti–B-Cell Maturation Antigen Chimeric Antigen Receptor Cause Remissions of Poor-Prognosis Relapsed Multiple Myeloma. *J Clin Oncol*. 2018;36(22):JCO.2018.77.808. doi:10.1200/jco.2018.77.8084

7. Cohen AD, Garfall AL, Stadtmauer EA, et al. B cell maturation antigen-specific CAR T cells are clinically active in multiple myeloma. *J Clin Invest*. 2019;130. doi:10.1172/jci126397

8. Raje N, Berdeja J, Lin Y, et al. Anti-BCMA CAR T-Cell Therapy bb2121 in Relapsed or Refractory Multiple Myeloma. *N Engl J Med*. 2019;380(18):1726-1737; 1737. doi:10.1056/nejmoa1817226

9. Berdeja JG, Madduri D, Usmani SZ, et al. Ciltacabtagene autoleucel, a B-cell maturation antigen-directed chimeric antigen receptor T-cell therapy in patients with relapsed or refractory multiple myeloma (CARTITUDE-1): a phase 1b/2 open-label study. *The Lancet*. 2021;398(10297):314-324. doi:10.1016/S0140-6736(21)00933-8

10. Sadelain M, Brentjens R, Rivière I. The Basic Principles of Chimeric Antigen Receptor Design. *Cancer Discov*. 2013;3(4):388-398. doi:10.1158/2159-8290.CD-12-0548

11. Dhakal B, Hari PN, Usmani SZ, Hamadani M. Chimeric antigen receptor T cell therapy in multiple myeloma: promise and challenges. *Bone Marrow Transplant*. 2021;56(1):9-19. doi:10.1038/s41409-020-01023-w

12. Shah NN, Fry TJ. Mechanisms of resistance to CAR T cell therapy. *Nat Rev Clin Oncol*. 2019;16(6):372-385. doi:10/gfwr8w

13. Brown CE, Mackall CL. CAR T cell therapy: inroads to response and resistance. *Nat Rev Immunol*. 2019;19(2):1. doi:10.1038/s41577-018-0119-y

14. Friedrich MJ, Neri P, Kehl N, et al. The pre-existing T cell landscape determines the response to bispecific T cell engagers in multiple myeloma patients. *Cancer Cell*. Published online 2023. doi:10.1016/j.ccell.2023.02.008

15. Gayoso A, Shor J. JonathanShor/DoubletDetection: doubletdetection v4.2. Published online March 12, 2022. doi:10.5281/ZENODO.6349517

16. Wolf FA, Angerer P, Theis FJ. SCANPY: large-scale single-cell gene expression data analysis. *Genome Biol*. 2018;19(1):15. doi:10.1186/s13059-017-1382-0

17. Keenan BP, McCarthy EE, Ilano A, et al. Circulating monocytes associated with anti-PD-1 resistance in human biliary cancer induce T cell paralysis. *Cell Rep*. 2022;40(12):111384. doi:10.1016/j.celrep.2022.111384

18. Johnson WE, Li C, Rabinovic A. Adjusting batch effects in microarray expression data using empirical Bayes methods. *Biostatistics*. 2007;8(1):118-127. doi:10.1093/biostatistics/kxj037

19. Korsunsky I, Millard N, Fan J, et al. Fast, sensitive and accurate integration of single-cell data with Harmony. *Nat Methods*. 2019;16(12):1289-1296. doi:10.1038/s41592-019-0619-0

20. Traag VA, Waltman L, Van Eck NJ. From Louvain to Leiden: guaranteeing well-connected communities. *Sci Rep*. 2019;9(1):5233. doi:10.1038/s41598-019-41695-z

21. Becht E, McInnes L, Healy J, et al. Dimensionality reduction for visualizing single-cell data using UMAP. *Nat Biotechnol*. 2019;37(1):38-44. doi:10.1038/nbt.4314

22. Zeileis, Achim. ineq: Measuring Inequality, Concentration, and Poverty. https://CRAN.R-project.org/package=ineq

23. Love MI, Huber W, Anders S. Moderated estimation of fold change and dispersion for RNA-seq data with DESeq2. *Genome Biol*. 2014;15(12):550. doi:10.1186/s13059-014-0550-8

24. Finak G, McDavid A, Yajima M, et al. MAST: a flexible statistical framework for assessing transcriptional changes and characterizing heterogeneity in single-cell RNA sequencing data. *Genome Biol*. 2015;16(1):278. doi:10.1186/s13059-015-0844-5

25. Picelli S, Faridani OR, Björklund ÅK, Winberg G, Sagasser S, Sandberg R. Full-length RNA-seq from single cells using Smart-seq2. *Nat Protoc*. 2014;9(1):171-181. doi:10.1038/nprot.2014.006

26. Grabherr MG, Haas BJ, Yassour M, et al. Full-length transcriptome assembly from RNA-Seq data without a reference genome. *Nat Biotechnol*. 2011;29(7):644-652. doi:10.1038/nbt.1883

27. Bray NL, Pimentel H, Melsted P, Pachter L. Near-optimal probabilistic RNA-seq quantification. *Nat Biotechnol*. 2016;34(5):525-527. doi:10.1038/nbt.3519

28. Efremova M, Vento-Tormo M, Teichmann SA, Vento-Tormo R. CellPhoneDB: inferring cell–cell communication from combined expression of multi-subunit ligand–receptor complexes. *Nat Protoc*. 2020;15(4):1484-1506. doi:10.1038/s41596-020-0292-x

29. Waskom M. seaborn: statistical data visualization. *J Open Source Softw*. 2021;6(60):3021. doi:10.21105/joss.03021

30. Subramanian A, Tamayo P, Mootha VK, et al. Gene set enrichment analysis: A knowledge-based approach for interpreting genome-wide expression profiles. *Proc Natl Acad Sci*. 2005;102(43):15545-15550. doi:10.1073/pnas.0506580102

31. Hyrenius-Wittsten A, Su Y, Park M, et al. SynNotch CAR circuits enhance solid tumor recognition and promote persistent antitumor activity in mouse models. *Sci Transl Med*. 2021;13(591):eabd8836. doi:10.1126/scitranslmed.abd8836

32. Roman Galletto. Bcma (cd269) specific chimeric antigen receptors for cancer immunotherapy. https://patents.google.com/patent/US20170183418

33. Stoeckius M, Zheng S, Houck-Loomis B, et al. Cell Hashing with barcoded antibodies enables multiplexing and doublet detection for single cell genomics. *Genome Biol*. 2018;19(1):224. doi:10.1186/s13059-018-1603-1

34. Mimitou EP, Cheng A, Montalbano A, et al. Multiplexed detection of proteins, transcriptomes, clonotypes and CRISPR perturbations in single cells. *Nat Methods*. 2019;16(5):409-412; 412. doi:10.1038/s41592-019-0392-0

35. Kang HM, Subramaniam M, Targ S, et al. Multiplexed droplet single-cell RNA-sequencing using natural genetic variation. *Nat Biotechnol*. 2017;36(1):89. doi:10.1038/nbt.4042

36. Aran D, Looney AP, Liu L, et al. Reference-based analysis of lung single-cell sequencing reveals a transitional profibrotic macrophage. *Nat Immunol*. 2019;20(2):163-172. doi:10.1038/s41590-018-0276-y

37. Morrow JS. Toward a more normative assessment of maldistribution: the Gini Index. *Inq J Med Care Organ Provis Financ*. 1977;14(3):278-292.

38. Bashford-Rogers R, Palser AL, Huntly BJ, et al. Network properties derived from deep sequencing of human B-cell receptor repertoires delineate B-cell populations. *Genome Res*. 2013;23(11):1874-1884; 1884. doi:10.1101/gr.154815.113

39. Haradhvala NJ, Leick MB, Maurer K, et al. Distinct cellular dynamics associated with response to CAR-T therapy for refractory B cell lymphoma. *Nat Med*. Published online 2022:1-12. doi:10.1038/s41591-022-01959-0

40. Good Z, Spiegel JY, Sahaf B, et al. Post-infusion CAR TReg cells identify patients resistant to CD19-CAR therapy. *Nat Med*. Published online 2022:1-12. doi:10.1038/s41591-022-01960-7

41. Deng Q, Han G, Puebla-Osorio N, et al. Characteristics of anti-CD19 CAR T cell infusion products associated with efficacy and toxicity in patients with large B cell lymphomas. *Nat Med*. 2020;26(12):1878-1887. doi:10.1038/s41591-020-1061-7

42. Dhodapkar KM, Cohen AD, Kaushal A, et al. Changes in Bone Marrow Tumor and Immune Cells Correlate with Durability of Remissions Following BCMA CAR T Therapy in Myeloma. *Blood Cancer Discov*. 2022;3(6):490-501. doi:10.1158/2643-3230.bcd-22-0018

43. Oh DY, Kwek SS, Raju SS, et al. Intratumoral CD4+ T Cells Mediate Anti-tumor Cytotoxicity in Human Bladder Cancer. *Cell*. 2020;181(7):1612-1625.e13. doi:10.1016/j.cell.2020.05.017

44. Melenhorst JJ, Chen GM, Wang M, et al. Decade-long leukaemia remissions with persistence of CD4+ CAR T cells. *Nature*. 2022;602(7897):503-509. doi:10.1038/s41586-021-04390-6

45. Park BV, Freeman ZT, Ghasemzadeh A, et al. TGFβ1-Mediated SMAD3 Enhances PD-1 Expression on Antigen-Specific T Cells in Cancer. *Cancer Discov*. 2016;6(12):1366-1381. doi:10.1158/2159-8290.CD-15-1347

46. Alabanza LM, Xiong Y, Vu B, et al. Armored BCMA CAR T Cells Eliminate Multiple Myeloma and Are Resistant to the Suppressive Effects of TGF-β. *Front Immunol*. 2022;13:832645. doi:10.3389/fimmu.2022.832645

47. Narayan V, Barber-Rotenberg JS, Jung IY, et al. PSMA-targeting TGFβ-insensitive armored CAR T cells in metastatic castration-resistant prostate cancer: a phase 1 trial. *Nat Med* 2022;28:724–734. https://doi.org/10.1038/s41591-022-01726-1.

Table 1: Patient's characteristics

Characteristic	Total (*n*=15)
Age, median (range), years	66 (34-74)
Male, *n* (%)	6 (40)
ECOG PS 0, *n* (%)	9 (60)
High risk cytogenetics[a], *n* (%)	8 (53)
BM PC >= 50%[b]	9 (69)
extramedullary disease, *n* (%)[c]	5 (55)
Prior anti-myeloma regimens, median (range)	6 (1-12)
Penta-refractory[d], *n* (%)	14 (93)
Prior ASCT, *n* (%)	14 (93)
Bridging therapy, *n* (%)	8 (53)

[a] del17p, t(4:14), t(14:16), 1q abnormalities

[b] % of 13 patients with adequate BM sample for evaluation

[c] % of 9 patients with PET-CT scans at baseline

[d] exposure or refractoriness to lenalidomide, pomalidomide, bortezomib, carfilzomib and daratumumab or isatuximab

Figure Legends

Figure 1: T cell states in myeloma and healthy age-matched controls. (A) Uniform manifold approximation and projection (UMAP) of total 690,939 T cells with annotated cell states. (B) Violin plot of normalized expression of selected representative genes for each cell state. (C) Density map of T cells from healthy controls (HC) and multiple myeloma (MM) patients. (D) Bar plot showing proportions of each cell state in HC and MM. Significance level was determined using Wilcoxon rank-sum test ($p < 0.001$). (E) Heatmap of normalized expression of selected differentially expressed genes between HC and MM.

Figure 2: Annotated CAR-T cells from 15 myeloma patients, their cell states, and TCR clonality. (A) Scheme showing annotation of CAR-T cells by de novo transcriptome assembly and targeted amplification. (B) Uniform manifold approximation and projection (UMAP) of 690,939 T cells with projection of annotated CAR-T cells (n = 100,157). (C) Fraction of CD4+ and CD8+ CAR-T over time (mean $\pm$ SE). (D) Bar plot showing proportions of annotated CAR-T cell states. Significance level was determined using Wilcoxon rank-sum test ($p < 0.001$). (E) Gini coefficients (mean $\pm$ SE) for nonCAR-T and CAR-T cells, by CD4+ and CD8+, over time. Baseline = prior to CAR-T infusion, early = day 14 and day 30 post – infusion, late = day $\geq$ 90 post – infusion. (F) Pie charts of expanded CAR-T clonotypes (same TCR clonotype in >1 cell), by CD4+ and CD8+.

Figure 3: Annotated CAR-T cells from 15 myeloma patients, their cell states, and TCR clonality. Involved serum free light chain (FLC) levels of myeloma patients over time after CAR-T cell therapy (day 0 = CAR-T infusion), by group. TR = transient responders, DR = durable responders. Statistical significance is marked by asterix, and determined by Wilcoxon rank-sum test with $p = 0.0113$. (B) Uniform manifold approximation and projection (UMAP) of T cells, with projection of annotated CAR-T cells from TR and DR groups at different time points (days) after infusion. (C) Bar plot showing the sum of CAR-T cells from n = 15 patients, by group, at different time points (days) post-infusion. (D) Bar plots showing CAR-T cells (mean $\pm$ SE) at different cell states, by group. Statistical significance is marked by asterix, and determined by Wilcoxon rank-sum test ($p = 0.030$) (E) Volcano plots showing differentially expressed genes between patient groups (DR vs. TR) in CD4+ CAR-T cells and CD8+ CAR-T cells. Annotated genes in red have a statistically significant ($p < 0.05$) fold

change (FC) >1.5. (F) Dot plots showing normalized expression of cytotoxicity and exhaustion genes in CD4+ and CD8+ CAR-T cells, by group. Dot size is proportional to fraction of cells.

Figure 4: Cytotoxic and exhausted CD4+ CAR-T cells harboring interferon gamma signature are identified preferentially in patients with transient response to therapy. (A) Density map of cytotoxicity and exhaustion gene signature scores for CD4+ and CD8+ CAR-T, by group. Cell fractions (%) are annotated in each quadrant. HC = healthy controls, TR = transient responders, DR = durable responders. (B) Bar plot showing CD4+ CAR-T cell fraction (mean % $\pm$ SE) of "double positive" cytotoxic and exhausted cells derived from the top right quadrant in panel B, by group. Statistical significance is marked by asterix, and determined by Wilcoxon rank-sum test (p = 0.03) (C) Box plot showing regulatory CAR-T cells (CAR-Treg) fraction (median % $\pm$ 1.5 IQR), by group. (D) Enrichment score (see methods) for interferon γ (IFNG) pathway of CD4+ CAR-T cells from DR group vs TR group. (E) Dot plots showing normalized expression of genes related to interferon γ (IFNG) pathway in CD4+ CAR-T cells, by group. Dot size is proportional to fraction of cells.

Figure 5: TGFβ is linked to interaction of non-classical monocytes in the myeloma niche might interact with CD4+ CAR-T via blunting their killing capacity of malignant plasma cells. (A) Uniform manifold approximation and projection (UMAP) of CD14+ myeloid cells with annotated cell states. (B) Violin plots showing normalized expression of selected genes for each cell state. (C) Box plot showing the proportions of CD14+ myeloid cells (median % $\pm$ IQR) of each cell state, by group. Statistical significance is marked by asterix, and determined by Wilcoxon rank-sum test ($p < 0.001$). HC = healthy controls, TR = transient responders, DR = durable responders. (D) Enrichment score (see methods) for TGFβ pathway of CD4+ CAR-T cells from DR group vs. TR group. (E) Dot plots showing normalized expression of genes related to TGFβ pathway in CD4+ CAR-T cells, by group. Dot size is proportional to fraction of cells. (F) Scheme depicting experimental design of CD4+ CAR-T cells *in vitro* killing assay performed by co-culture with myeloma cell line MM1.S, with and without TGFβ. (G) Bar plot showing killing efficacy of CD4+ CAR-T cells (number of cancer cells killed per CD4+ CAR-T cell) after 3 weeks of co-culture with myeloma cell line MM1.S, with or without TGFβ. (H) Frequency of CD4+ CAR T cells expressing 3 exhaustion markers (PD-1, TIM3, CD39) after

repetitive stimulation. (I) Flow cytometry histogram of PD-1 mean fluorescence intensity (MFI) of CD4+ CAR-T cells from 2 donors after 3 weeks of co-culture with myeloma cell line MM1.S, with or without TGFβ.

Figure 1

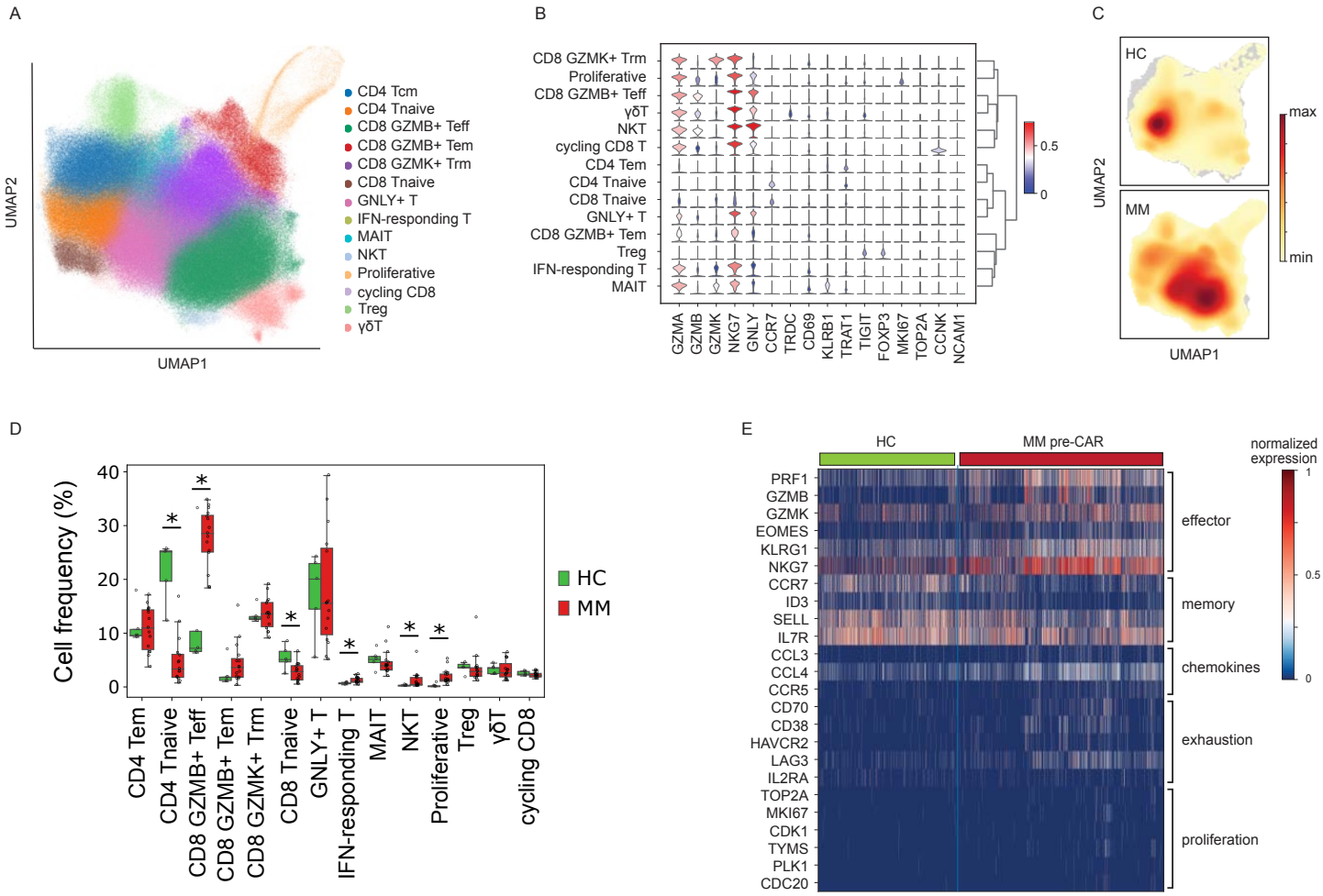

Figure 2

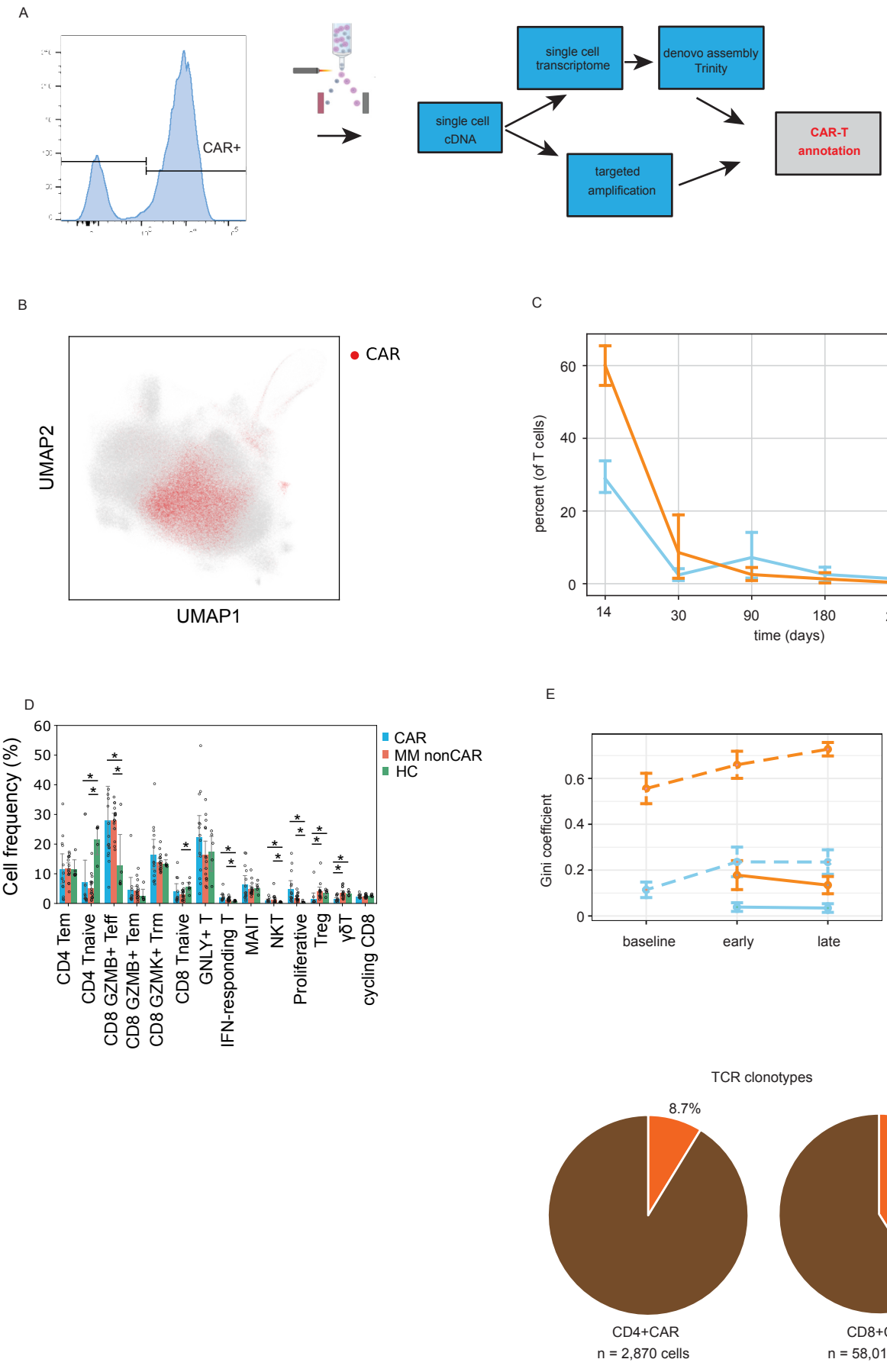

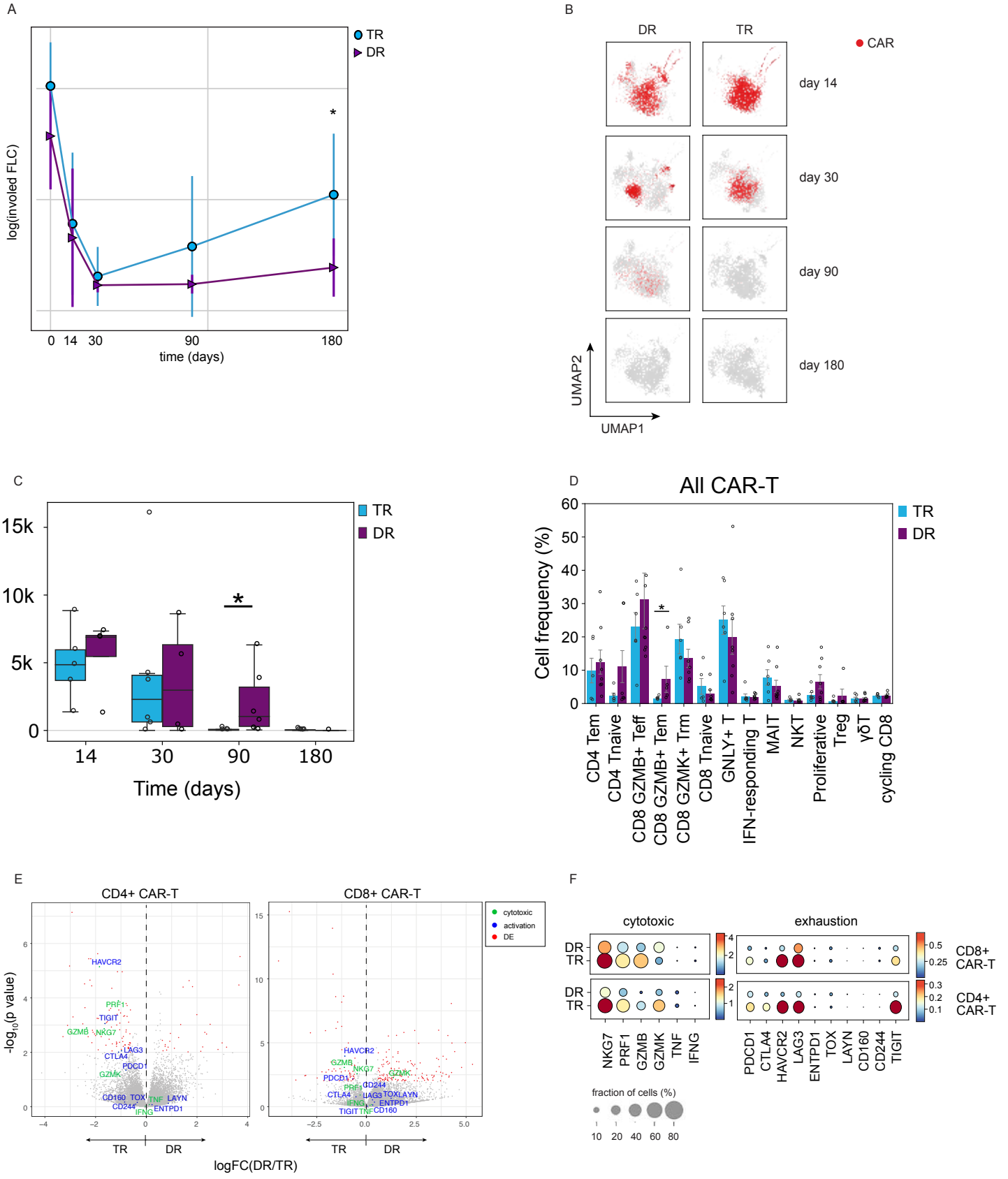

Figure 4

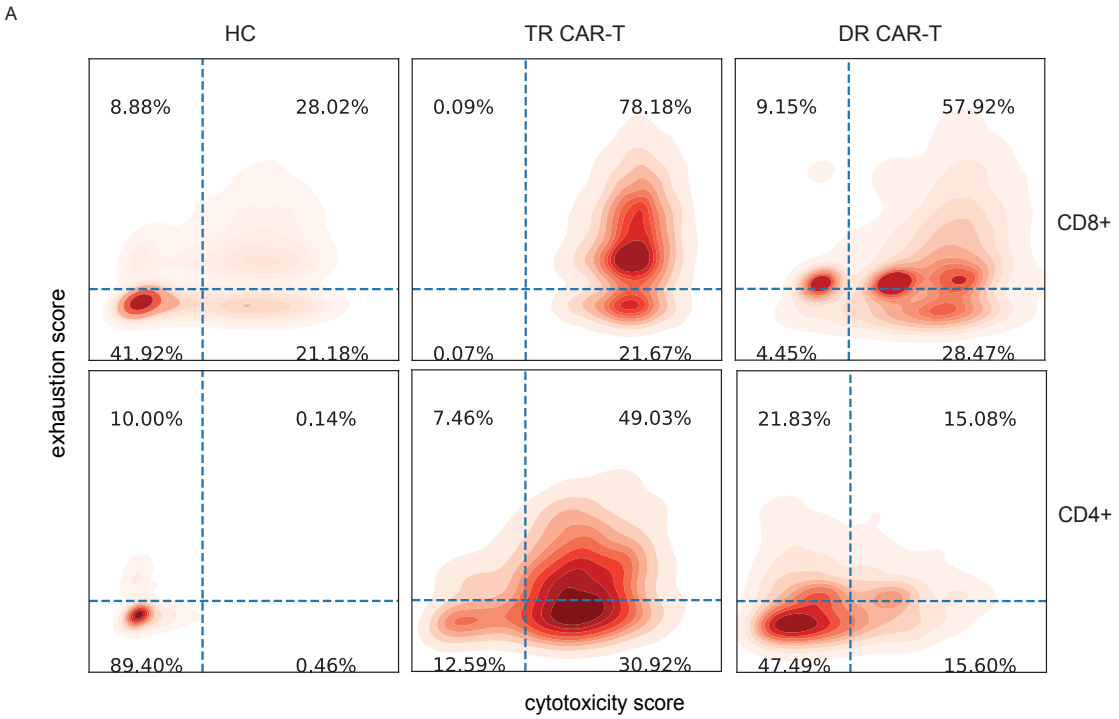

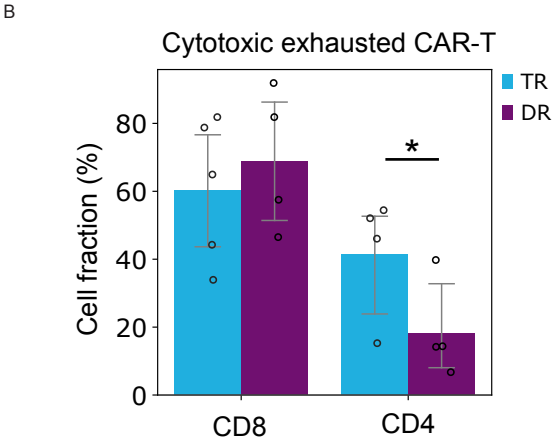

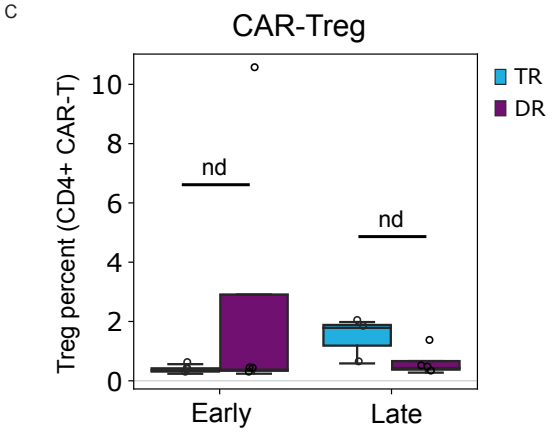

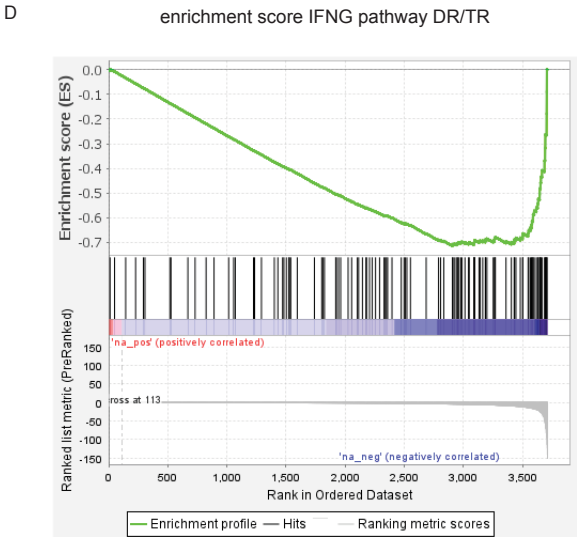

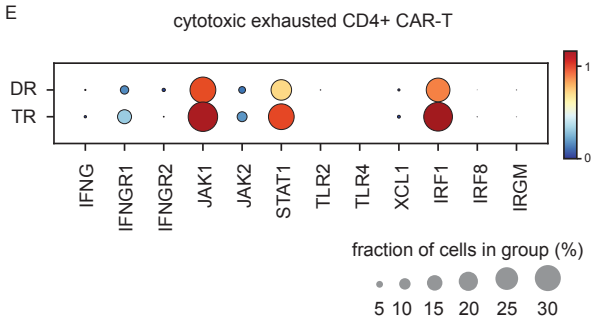

Figure 5